Tunable terahertz radiation from graphene induced by moving electrons

Tianrong Zhan,[1,2,*] Dezhuan Han,[1,3] Xinhua Hu,[4] Xiaohan Liu,[1] Siu-Tat Chui,[2] and Jian Zi[1,†]

[1]*Department of Physics, Key Laboratory of Micro and Nano Photonic Structures (Ministry of Education), and Key Laboratory of Surface Physics, Fudan University, Shanghai 200433, People's Republic of China*

[2]*Bartol Research Institute, University of Delaware, Newark, Delaware 19716, USA*

[3]*Department of Applied Physics, College of Physics, Chongqing University, Chongqing 400044, People's Republic of China*

[4]*Department of Materials Science and Laboratory of Advanced Materials, Fudan University, Shanghai 200433, People's Republic of China*

(Received 4 September 2013; revised manuscript received 27 May 2014; published 20 June 2014)

Based on a structure consisting of a single graphene layer situated on periodic dielectric gratings, we show theoretically that terahertz radiation can be generated by low-energy electron bunches moving atop the graphene layer. The THz emission arises from graphene plasmons excited efficiently by the moving electrons. We find that the radiation intensity can be strongly enhanced due to the local field enhancement of graphene plasmons arising from their low losses and high confinement. Importantly, the radiation frequency can be tuned over a wide spectral range by varying the Fermi level of the graphene layer. Our results could find applications in developing tunable and miniature free-electron terahertz radiation sources.

DOI: 10.1103/PhysRevB.89.245434 PACS number(s): 78.67.Wj, 42.72.−g, 73.20.Mf

I. INTRODUCTION

Graphene photonics and optoelectronics have attracted intense research interest in recent years [1]. This is because graphene possesses exceptional electronic and optical properties due to its unique electronic band structure, i.e., the existence of Dirac cones [2]. Indeed, a variety of novel applications such as broadband photodetectors, optical modulators, and ultrafast lasers have been proposed [1]. Interestingly, graphene can support plasmons with frequencies in terahertz (THz) and midinfrared regimes [3,4]. Compared with surface plasmons in noble metals [5], graphene plasmons (GPs) exhibit remarkable properties such as strong slow-wave effects, extreme light confinement, and low Ohmic losses with a further advantage of being tunable through electrostatic gating or chemical doping [6–8]. These features make graphene a promising material for active plasmonic devices [8], which could find applications in transformation optics [9], metamaterials [10], light harvesting [11,12], and nonlinear optics [13].

Terahertz radiation with frequencies from 0.1 to 30 THz has attracted increasing attention due to its wide range of potential applications [14]. However, a lack of desired sources of THz radiation limits the realization of such applications. During the past decade, many approaches, including optically pumped solid-state devices, quantum cascade lasers, diodes, and free-electron devices, have been investigated for the development of THz sources [15]. Free-electron THz sources, wherein radiation occurs as moving electrons interact typically with a perturbing element [16–18], are of particular interest owing to their high power and continuous tunability by varying electron energies [15]. However, traditional free-electron THz sources usually require relativistic electron energies, leading to the difficulty in reducing their size while retaining their wide tunability, which constitutes a great challenge for the applications of such sources. Progress in this direction has been made by exploiting radiation emission in photonic slow-wave structures driven by relative low-energy electrons. Recent studies include terahertz Cherenkov radiation in resonant dielectric-loaded waveguides [17,19,20] and light emission at visible frequencies in nanostructured plasmonic structures [21–24].

In this paper, we show theoretically that intense and tunable THz radiation can be generated by low-energy electron bunches (∼1 keV) moving atop a graphene layer situated on periodic dielectric gratings. The underlying physics lies in the fact that low-energy moving electrons can efficiently excite GPs of THz frequencies, and GPs in turn can be transformed into free-space radiation by the grating when satisfying the phase matching condition. We find that the radiation intensity is strongly enhanced around GP excitation frequencies. Based on a self-consistent electromagnetic theory for the interaction of moving electrons with GPs, we reveal that the radiation enhancement can be attributed to the local field enhancement of GPs arising from their low losses and high confinement. We further show that the radiation frequency can be tuned over a wide spectral range by varying the Fermi energy of the graphene layer in conjunction with changing the grating periodicity.

II. EXCITATION OF GPs BY MOVING ELECTRONS

We start by considering an electron bunch moving atop a graphene layer on a dielectric substrate. Suppose the electron bunch moves at a constant velocity v in the x direction atop the graphene layer by a distance b. For simplicity, the electron bunch is assumed to be uniform along y with a line charge density ρ. The moving electrons can be treated as a source with a current density $\mathbf{J}(\mathbf{r},t) = \hat{\mathbf{x}}\rho v\delta(z-b)\delta(x-vt)$, which may induce a transverse-magnetic electromagnetic (EM) wave of the form $e^{i(k_x x + k_z|z-b|)}$ with its magnetic field polarized along y in the frequency domain (see Note 1 in the Supplemental Material [25]), representing a plane wave of a wave vector $k_x\hat{\mathbf{x}}+\mathrm{sgn}(z-b)k_z\hat{\mathbf{z}}$, where $k_x = \omega/v$, $k_z = \omega\sqrt{1/v_p^2 - 1/v^2}$, and ω and v_p are the angular frequency and phase velocity of light in an ambient medium, respectively. Obviously, Cherenkov radiation occurs when $v \geqslant v_p$ [26], whereas no

*phystrzhan@gmail.com
†jzi@fudan.edu.cn

radiation is expected when $v < v_p$ since k_z is purely imaginary and therefore the induced EM wave is evanescent.

However, we will show that the evanescent EM wave induced by moving electrons can efficiently excite GPs in a graphene layer. Doped or gated graphene can support GPs that propagate on a graphene layer with associated EM fields strongly confined and enhanced near its surface [3,4,6,7], as shown in Fig. 1(b). GPs possess slow phase velocity, which is approximated by $v_{\rm gp}/c \simeq \frac{4\alpha}{1+\varepsilon_d}\frac{E_F}{\hbar\omega}$ in the nonretarded regime ($k_{\rm gp} \gg \omega/c$) [6,7], where $k_{\rm gp}$ is the GP wave vector, E_F is the Fermi energy, ε_d is the permittivity of the dielectric substrate, α is the fine-structure constant, and c is the light speed in air. Note that $v_{\rm gp}/c$ can be of the order of 10^{-1}–10^{-2} and further tuned by varying E_F at THz frequencies, suggesting that graphene can be used as a tunable slow-wave structure.

When the electron bunch moving atop a graphene layer, the induced evanescent EM wave can excite GPs if satisfying the phase matching condition [27,28], namely,

$$k_{\rm gp}(\omega) = \omega/v. \tag{1}$$

Clearly, Eq. (1) is equivalent to $v_{\rm gp}(\omega) = v$, which is satisfied at intersections of GP dispersion curves with electron beam lines. Thus, the GP modes excited are given by $\omega_{\rm gp} \simeq \frac{4\alpha}{1+\varepsilon_d}\frac{E_F}{\hbar v/c}$. As shown in Fig. 1(a), for $E_F = 0.4$ eV, the frequency of the excited GP is about 10 THz with $v = 0.057c$ (corresponding to a rather low electron energy 0.832 keV). The excited GP frequency can be tuned by adjusting E_F, e.g., about 24.9 THz for $E_F = 1.0$ eV.

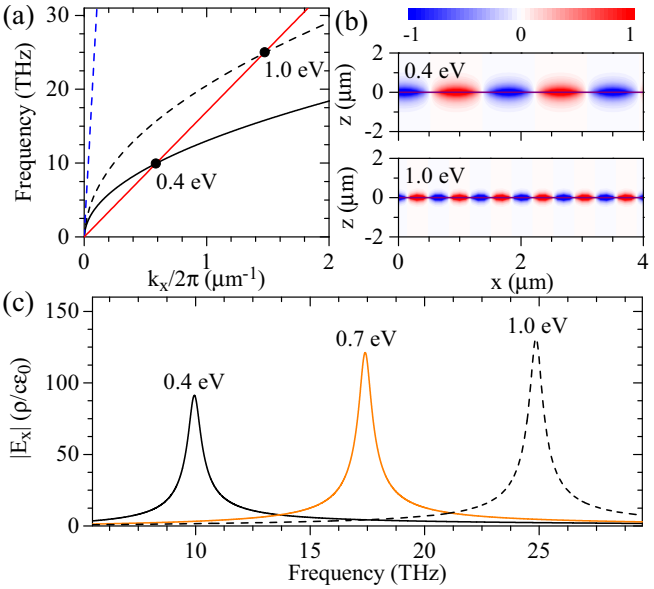

FIG. 1. (Color online) Excitation of GPs in a graphene layer at $z = 0$ on a dielectric substrate with $\varepsilon_d = 4$ by an electron bunch moving with constant velocity v in the x direction and at $z = b$. The graphene has an intrinsic relaxation time of $\tau = 0.6$ ps throughout this work. (a) Dispersion curves of GPs at different E_F (black lines). The red solid line shows the electron beam line $\omega/k_x = v$ with $v = 0.057c$, and the blue dashed line represents the light line $\omega/k_x = c$, where c is the light speed in air. (b) Distribution of field $\mathrm{Re}(E_x)$ for two GP modes [dots in (a)]. (c) $|E_x(z = 0)|$ vs frequency for $v = 0.057c$ and $b = 0.1$ μm at different E_F.

To present a quantitative description and investigate the excitation efficiency, one can recall that plasmon excitation by moving electrons can be related to electron energy losses suffered along their trajectory due to the interaction of the electrons with the induced electric field $\mathbf{E}_x^{\rm ind}$ in the presence of the graphene layer, which is given by $W_{\rm EEL} = -\int dt \mathbf{J}(\mathbf{r},t)\cdot\mathbf{E}_x^{\rm ind}(\mathbf{r},t)$, describing the work done by $\mathbf{E}_x^{\rm ind}$ back on the electrons [27]. To examine the plasmon excitation, it is convenient to obtain in the frequency domain $W_{\rm EEL} = -\frac{1}{\pi}\int_0^\infty d\omega\,\mathrm{Re}[\mathbf{J}^*(\mathbf{r},\omega)\cdot\mathbf{E}_x^{\rm ind}(\mathbf{r},\omega)]$, where $\mathbf{J}(\mathbf{r},\omega) = \hat{\mathbf{x}}\rho\delta(z-b)e^{i\frac{\omega}{v}x}$. Intuitively, since GPs exhibit strong local electric field enhancement, one can expect that $\mathbf{E}_x^{\rm ind}$ can be enhanced under the phase matching condition of Eq. (1), leading to the enhancement of the electron energy loss and thus the GP excitation efficiency. To corroborate this, we can obtain $\mathbf{E}_x^{\rm ind}$ rigorously by solving Maxwell equations when considering the EM fields associated with the moving electrons in air as incident fields upon the graphene layer [29–31]. In the presence of the graphene layer, reflection and transmission should be expected, yielding the total electric fields as (see Note 2 in the Supplemental Material [25])

$$\mathbf{E}_x^{\rm ind}(\mathbf{r},\omega) \equiv \zeta e^{ik_x x}\begin{cases} e^{-\gamma_1|z-b|} - re^{-\gamma_1(z+b)}, & z > 0, \\ t\eta e^{-\gamma_1 b}e^{\gamma_2 z}, & z < 0, \end{cases} \tag{2}$$

where $\zeta = -i\frac{\rho}{2c\varepsilon_0}\frac{\gamma_1}{k_0}$, $r = \frac{1-\eta+\xi}{1+\eta+\xi}$ and $t = \frac{2}{1+\eta+\xi}$ are reflection and transmission coefficients of the graphene layer, respectively, $\eta = \gamma_2/(\varepsilon_d\gamma_1)$, $\xi = i\sigma_{\rm gp}\gamma_2/(\varepsilon_0\varepsilon_d\omega)$, $\gamma_1 = \sqrt{k_x{}^2 - k_0{}^2}$, $\gamma_2 = \sqrt{k_x{}^2 - \varepsilon_d k_0{}^2}$, $k_x = \omega/v$, and $k_0 = \omega/c$. At THz frequencies, graphene conductivity simplifies to $\sigma_{\rm gp}(\omega) = 4\alpha\epsilon_0 c\frac{iE_F}{\hbar(\omega+i/\tau)}$ on the condition that $E_F \gg k_B T$, where τ is the relaxation time, T is the temperature, and k_B is the Boltzmann constant [6].

From Eq. (2), $\mathbf{E}_x^{\rm ind}$ can exhibit a resonance at the pole of the reflection (transmission) coefficient under the condition $\eta + \xi = -1$, corresponding exactly to the phase matching condition of Eq. (1), i.e., the excitation of GPs [32]. As a result, the induced EM fields near the graphene layer can be considerably enhanced around GP resonant frequencies, as shown in Fig. 1(c). The enhancement factor can be explicitly related to the properties of excited GPs. To see this, at GP resonant frequencies, we can reduce Eq. (2) in the nonretarded regime to

$$\mathbf{E}_x^{\rm ind}(z = 0,\omega_{\rm gp}) \simeq \frac{2\rho}{c\varepsilon_0(1+\varepsilon_d)}\frac{\omega_{\rm gp}\tau}{k_0/\gamma_1}e^{ik_x x}e^{-\gamma_1 b}. \tag{3}$$

Note that, while $\omega_{\rm gp}\tau$ can be about 11 and 110 with $\tau \sim 0.6$ ps at frequencies of 3 and 30 THz, respectively, $1/\gamma_1$ is the GP confinement length along z and $k_0/\gamma_1 \simeq v_{\rm gp}/c$ is of the order of 10^{-1}–10^{-2}. Therefore, the excitation efficiency of GPs by moving electrons can be strongly enhanced due to low losses and high confinement of GPs. Note that efficiently exciting GPs with free-space radiation is typically challenging because there is a large wave-vector mismatch between GPs and free-space radiation due to the high confinement of GPs. However, the results here show that low-energy electrons could be used to efficiently excite GPs by taking advantage of their high confinement in addition to their low losses. These results are distinct from previous studies [28] in which Eq. (3) accounts

for the effect of losses in graphene and could provide a solid link between the GP excitation efficiency and the properties of GPs.

III. RADIATION EMISSION FROM GPs EXCITED BY MOVING ELECTRONS

As shown, moving electrons atop a graphene layer can efficiently excite GPs. However, the excited GPs cannot couple into free-space radiation due to the wave-vector mismatch between them. To transform GPs into free-space radiation, we consider a graphene layer situated on a periodic dielectric grating, as schematically shown in Fig. 2(a). The grating consists of one-dimensional (1D) periodic grooves on a dielectric substrate. The groove has period a, thickness h, and filling fraction f. In the following discussions, the dielectric substrate has $\varepsilon_g = 11.6$, and other parameters are $a = 1.3\ \mu$m, $h = 0.4\ \mu$m, $f = 0.7$, and $b = 0.1\ \mu$m.

The underlying physics for the transformation of excited GPs into free-space radiation stems from the fact that the wave-vector mismatch between GPs and free-space radiation can be compensated by reciprocal lattice vectors of the grating under the phase matching condition [33], namely,

$$k_{gp} + 2\pi m/a = \begin{cases} k_0 \sin\theta_+, & z > 0, \\ \sqrt{\varepsilon_g} k_0 \sin\theta_-, & z < 0, \end{cases} \tag{4}$$

where m is the diffraction order of the grating and θ is the radiation angle with respect to z. Different branches of diffraction order m represent band foldings. Consequently, the GP dispersion is now characterized by a well-defined band structure, as shown in Fig. 2(b), which is obtained numerically by a scattering matrix method [33]. Band gaps appear at the Brillouin zone center and boundaries due to multiple Bragg scatterings arising from the introduced periodicity. As a result, GP modes can reside above the light line, and therefore radiate into free space when excited by moving electrons [Fig. 2(c)], giving rise to free-electron-induced radiation emission [21–24]. Such radiation emission belongs to a special kind of diffraction radiation due to the excitation of resonant modes in photonic structures by the evanescent EM fields associated with moving electrons [27]. Note that Smith-Purcell radiation can also occur due to diffraction of the grating with its angular dispersion determined by electron beam lines folded above the light line (see Note 3 in the Supplemental Material [25]).

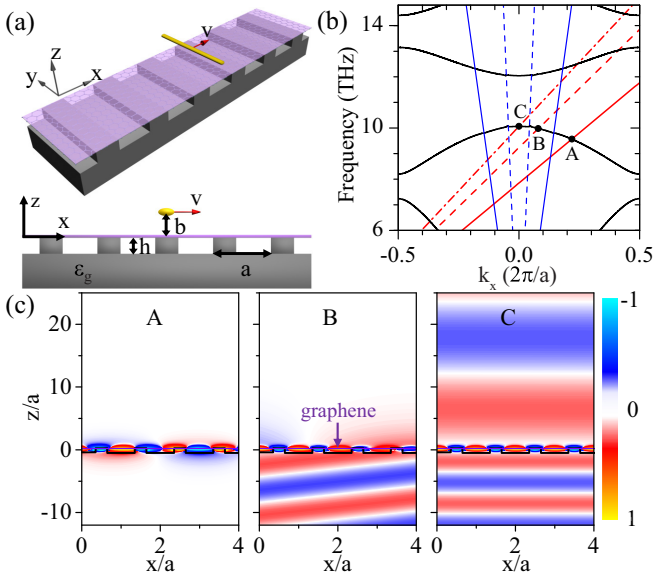

FIG. 2. (Color online) (a) Three-dimensional (3D) view (upper panel) and side view (lower panel) of an electron bunch moving atop a graphene layer on an 1D dielectric grating. (b) Dispersion curves (black solid lines) of GPs for the structure in (a). Red solid, dashed, and dashed-dotted lines show folded electron beam lines $\omega/(k_x + 2\pi/a) = v$ with $v = 0.034c$, $0.04c$, and $0.0436c$, respectively. Blue dashed and solid lines represent light lines $\omega/k_x = c$ (air) and $\omega/k_x = c/\sqrt{\varepsilon_g}$ (substrate), respectively. (c) Distribution of field $\mathrm{Re}(E_x)$ at frequencies of modes A, B, and C excited by the electron bunch with corresponding v in (b) and $b = 0.1\ \mu$m. The black solid lines in (c) depict the profile of the grating.

The angular dispersion of the radiation from excited GPs is determined by GP bands above the light line through Eq. (4), as shown in Fig. 2(c), which plots the radiation patterns of GPs at different positions in the Brillouin zone. In this study, we focus on GP modes in the first folded band ($m = \pm 1$); GP modes in other bands can be analyzed similarly based on Eq. (4). Note that there are two kinds of light lines, one for the air side and the other for the substrate side. For the mode A with $v = 0.034c$, since it is below the light line of both air and substrate, no free-space radiation can occur as expected. However, the mode B with $v = 0.04c$, since it resides between the light line of air and substrate, can give rise to free-space radiation toward the substrate side at an oblique angle determined by Eq. (4). Interestingly, as the mode C with $v = 0.0436$ resides at the center of the Brillouin zone, it can generate free-space radiation normal to the grating toward both sides.

To characterize quantitatively the radiation induced by the moving electrons, we obtain the spectral density of radiated energy from the Poynting vector of the radiated waves (see Note 3 in the Supplemental Material [25])

$$\frac{d}{d\omega} W_\pm = \frac{\rho^2}{4\pi\varepsilon_0 c} \frac{\cos(\theta_\pm)}{\sqrt{\varepsilon_\pm}} |R_\pm(\omega)|^2 e^{-2\gamma_1 b}, \tag{5}$$

where the plus (minus) sign stands for the air (substrate) side, and R is referred to as the radiation factor, with $R_+(R_-)$ being the reflection (transmission) coefficient of the structure, which can be calculated numerically by the scattering matrix method [29].

Figures 3(a)–3(c) show the radiation intensity $|R_\pm(\omega)|^2$ as a function of frequency. From Eq. (4), the radiation intensity is also plotted as a function of radiation angle $|R_\pm(\theta)|^2$, shown in Figs. 3(d)–3(f). For $v = 0.034c$ [Fig. 3(a)], since the excited GP mode [mode A in Fig. 2(b)] lies below the light line of both air and substrate, it cannot contribute to free-space radiation. Only a continuum of Smith-Purcell radiation from the grating is observed toward both sides [16,29] . Also, the radiation is distributed over a broad angular range [Fig. 3(d)]. In contrast, for $v = 0.04c$, a prominent resonant peak in the radiation spectra can be observed toward the substrate side [Fig. 3(b)], corresponding exactly to the excited GP mode [mode B in Fig. 2(b)]. Interestingly, the radiation toward the substrate side is highly directional at an oblique angle, as shown in Fig. 3(e).

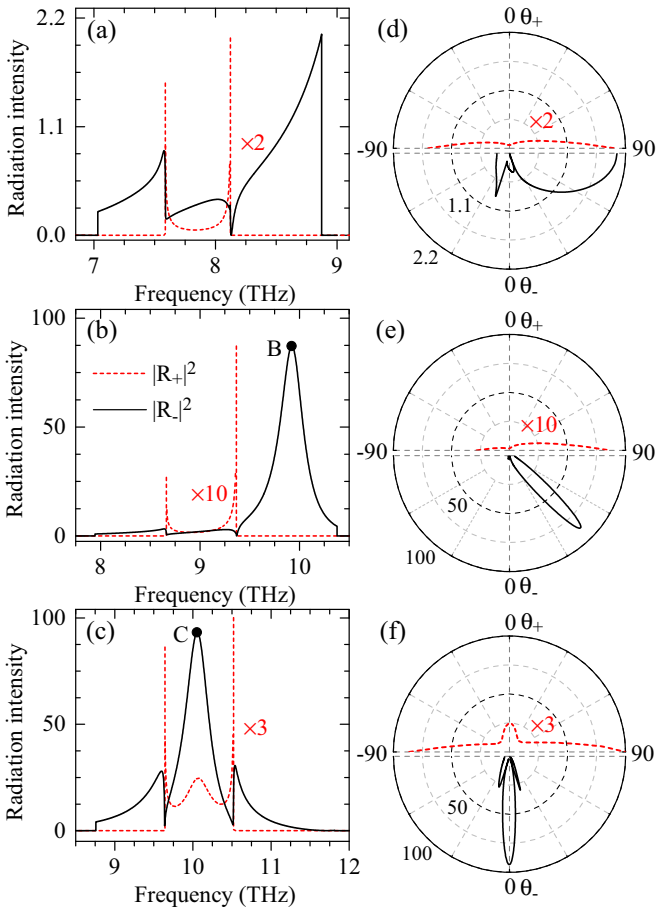

FIG. 3. (Color online) Radiation intensity $|R_+|^2$ toward the air side (red dashed lines) and $|R_-|^2$ toward the substrate side (black solid lines) vs frequency (left panels) and observation angle θ (right panels) for the setup shown in Fig. 2(a). The velocity of electron bunch is $v = 0.034c$ in (a) and (d), $0.04c$ in (b) and (e), and $0.0436c$ in (c) and (f). The modes B and C in (b) and (c) are related to those in Fig. 2, respectively.

Note that Smith-Purcell radiation still exists toward both sides but with much lower intensity compared with that from the excited GP. When $v = 0.0436c$ [Fig. 3(c)], prominent resonant peaks at the excited GP frequency [mode C in Fig. 2(c)] can be observed toward both the air and substrate sides in the radiation spectra, leading to highly directional radiation normal to the grating toward both sides [Fig. 3(f)].

The results here show that highly directional radiation can be generated from excited GPs by moving electrons and the radiation intensity can be strongly enhanced around GP resonant frequencies. We will show with the help of a self-consistent electromagnetic theory based on a modal expansion that the radiation enhancement is also directly related to the local electric field enhancement of GPs.

A. Radiation enhancement from excited GPs

To gain a deeper insight into the physics of the strongly enhanced radiation from excited GPs, we develop a self-consistent electromagnetic theory for the interaction of moving electrons with GPs based on the assumption that the induced EM fields can be expressed in the basis of GP modes around GP resonant frequencies ω_{gp} (see Appendix A). Since the intensity of the radiation from excited GPs is dominant over that of the Smith-Purcell radiation, we further assume that the electron energy loss is totally converted into GPs around ω_{gp} and they in turn radiate into free space. Obviously, the radiation enhancement can be attributed to the induced local electric field enhancement of GPs based on this theory. The theory can provide a closed-form expression for the radiation intensity as

$$|R_\pm(\omega)|^2 = F\frac{\omega_{gp}^2}{4Q^2(\omega-\omega_{gp})^2+\omega_{gp}^2}\frac{Q}{Q_{r,\pm}}\frac{\sqrt{\varepsilon_\pm}}{\cos(\theta_\pm)}, \quad (6)$$

where $F = \frac{2}{\pi}\frac{Q}{V/\lambda}$, $\lambda = 2\pi c/\omega_{gp}$, V describes the spatial confinement of GPs (see Appendixes A and B), Q is the total quality factor, $Q_{r,\pm}$ is the radiative contribution to Q due to the coupling of GPs to free space toward the air (substrate) side, and $Q/Q_{r,\pm}$ is the outcoupling factor representing the portion of energy converted into GPs that can be radiated into free space. These fitting parameters can emerge from our numerical calculations of the radiation intensity (see Appendix C), and they bear an intrinsic dependence on the geometrical and optical properties of the structures. We also apply this theory to investigate the excitation of GPs on the dielectric substrate, and it can reproduce the induced electric field given in Eq. (3) at GP resonant frequencies (see Note 4 in the Supplemental Material [25]).

Figures 4(a)–4(c) show the fitting of the numerical results to Eq. (6). There is a good agreement between them around GP resonant frequencies. $|R_\pm(\omega)|^2$ exhibits a Lorentzian line shape, reaching a maximum of $F\frac{Q}{Q_{r,\pm}}\frac{\sqrt{\varepsilon_\pm}}{\cos(\theta_\pm)}$ at GP resonant frequencies. Note that the maximum radiation intensity is linearly proportional to Q^2. Figure 4(d) presents the fitted value of Q, V/λ, and $Q/Q_{r,\pm}$ for different v. Interestingly, both Q and λ/V can be of the order of 10, suggesting that the radiation enhancement is due to large quality factors and

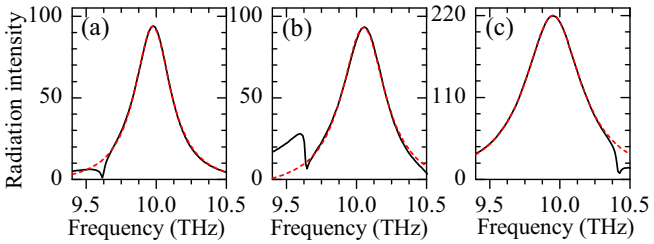

(d)

	v = 0.04c	v = 0.0436c	v = 0.0473c
Q	31.5	25.4	20.5
λ/V	3.4	6.9	13.1
$Q/Q_{r,-}$	0.31	0.21	0.31

FIG. 4. (Color online) (a)–(c) Numerical results of radiation intensity $|R_-|^2$ toward the substrate side (black solid lines) and their fitting to the theory of Eq. (6) (red dashed lines). The results are obtained for the setup shown in Fig. 2(a) with (a) $v = 0.04c$, (b) $v = 0.0436c$, and (c) $v = 0.0473c$. (d) Fitted value of Q, λ/V, and $Q/Q_{r,-}$ for different v.

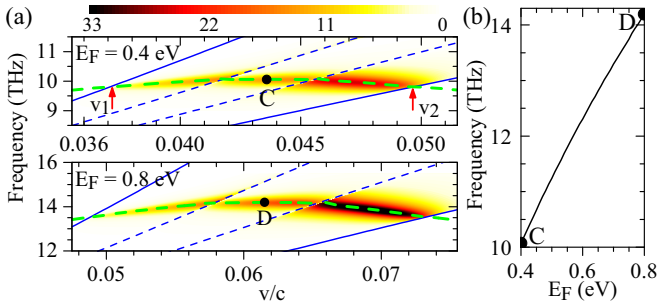

FIG. 5. (Color online) (a) Spectral density of radiated energy $dW_-/d\omega$ toward the substrate vs v and frequency for a setup with $b = 0$ as shown in Fig. 2(a). $dW_-/d\omega$ is of units of $\rho^2/\epsilon_0 c$ and plotted in a color scale form. Green dashed lines are obtained from Eq. (1). Blue dashed (blue solid) lines are obtained from intersection points of the red lines with blue dashed (blue solid) lines in Fig. 2(b). (b) Frequency of the excited GP at $k_x = 0$ [see Fig. 2(b)] vs E_F. The corresponding v can be calculated from $\omega/(k_x + 2\pi/a) = v$.

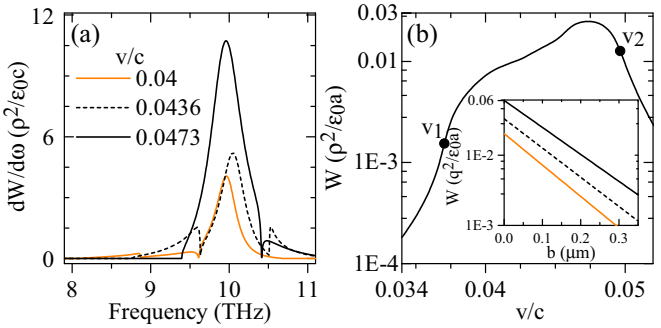

FIG. 6. (Color online) (a) Spectral density of radiated energy $dW_-/d\omega$ toward the substrate vs frequency, and (b) radiated energy W_- toward the substrate vs v for a setup with $b = 0.1$ μm as shown in Fig. 2(a). The inset to (b) plots the radiated energy W_- vs b for different v studied in (a). v_1 and v_2 in (b) correspond to those in Fig. 5(a), respectively.

high confinement of excited GPs. It is worth pointing out that $Q/Q_{r,-}$ is of the order of 0.2–0.3, indicating that the radiation enhancement is still limited by the low outcoupling factor due to optical losses in graphene. It can be shown that much larger radiation enhancement can be achieved for lower losses in graphene. Details about the dependence of the radiation enhancement on optical losses in graphene are discussed in Note 5 in the Supplemental Material [25].

B. Dependence of radiation emission on electron velocity and Fermi energy

Figure 5(a) shows the spectral density of radiated energy as a function of v and frequency for different E_F. We focus on the radiation toward the substrate side since its intensity is much larger than that toward the air side. For a given E_F, the radiation from excited GPs occurs over a narrow frequency range, showing a weak dependence on v. This weak dependence stems from the weak dispersion of GP bands above the light line due to the deep subwavelength nature of GPs [33]. However, the radiation peak shows a strong dependence on E_F. From Fig. 5(b), the peak frequency varies roughly from 10 to 14.2 THz as E_F is increased from 0.4 to 0.8 eV. The spectral range of the radiation can be further tuned by engineering the grating structure. For example, the peak frequency can be tuned from 14.8 to 23.4 THz as E_F is increased from 0.4 to 1.0 eV for $a = 0.6$ μm, $h = 0.3$ μm, and $f = 0.7$ (see Note 6 in the Supplemental Material [25]). Therefore, the radiation can be tuned over a wide frequency range by varying the Fermi level in combination with changing the periodicity of the grating.

C. Estimation of total radiated energy

By integrating the spectral density of Eq. (5) over frequency and radiation angle, the total radiated energy W can be obtained, shown in Fig. 6(b) as a function of v. The radiated energy is dominated over the velocity range where the excited GPs contribute to the radiation. For example, for $v = 0.0436c$, the radiated energy is $W = 1.26 \times 10^{-2}\rho^2/\epsilon_0 a$, nearly two orders of magnitude larger than $W = 1.81 \times 10^{-4}\rho^2/\epsilon_0 a$ for $v = 0.034c$, where only Smith-Purcell radiation occurs [Fig. 5(a)]. To evaluate quantitatively the radiated energy, we consider an electron bunch with $\rho = 100$ pC/cm. The total radiated energy is estimated to be $W = 1.099 \times 10^{-3}$ μJ/cm^2 for $v = 0.0436c$, corresponding to a peak power of 1.31 kW/cm^2 for a radiation pulse of 0.841 ps, where the pulse duration of the radiation is estimated from the spectral bandwidth of radiation peaks. The peak value of $dW/d\omega$ is found to be 0.0123 μJ/cm^2/THz at 10.05 THz.

IV. DISCUSSION

In our calculations, the intensity of radiation emission from GPs is mainly limited by the impurity- and phonon-limited relaxation time $\tau = 0.6$ ps (see Note 7 in the Supplemental Material [25]), which is estimated for $E_F = 0.4$ eV from the measured dc mobility $\mu = 1.5 \times 10^4$ cm^2/V s at room temperature [34]. While impurity scattering is the dominant factor limiting τ in low-quality graphene [35], τ can be improved in high-quality graphene which has been reported to achieve high mobility values, an order of magnitude larger than what is assumed in this paper [2,36,37]. On the other hand, graphene optical phonons significantly degrade τ for frequencies above $\omega_{\text{oph}} = 48.4$ THz [6,38]. However, the THz frequency regime of interest is below ω_{oph}. Therefore, intense radiation from GPs could be achieved in the THz regime.

We now consider the experimental implementation of our proposal. The fabrication of high-quality graphene and its integration with subwavelength dielectric gratings have already been demonstrated experimentally [34,39]. While subpicosecond electron bunches required in the THz regime can be obtained in the keV energy range with the state-of-the-art development of ultrafast pulsed electron sources based on photoionization or the photoelectric effect by employing femtosecond lasers [40–42], continuous electron beams from low-voltage electron microscopes could also be employed to realize the effect shown in this paper [21]. By taking advantage of the high resolution of electron microscopes, electron beams including both continuous and bunched ones can be directed parallel to the surface of a system over a distance on the nanometer scale [21,43]. Although charge

density in subpicosecond electron bunches with good beam quality may be limited, electron bunch trains with a high repetition rate could be used to further increase the radiation intensity [44].

In conclusion, we have theoretically shown that intense and tunable THz radiation can be generated due to radiation emission from GPs excited by low-energy electrons moving atop a graphene layer on periodic dielectric gratings. Based on a self-consistent electromagnetic theory for the interaction of moving electrons and GPs, we revealed that the radiation intensity can be strongly enhanced due to the electric field enhancement of GPs arising from their large quality factors and high confinement. We further showed that the dispersion relation of radiation emission from GPs is determined by GP band structures above the light line, leading to a weak dependence of the radiation emission on electron velocities due to the weak angular dispersion of GP bands above the light line. Importantly, the radiation frequency can be tuned by varying the Fermi level of the graphene layer, which can be changed flexibly via electrostatic gating or chemical doping, offering tunable terahertz radiation that can cover a wide spectral range. In the case of electrostatic gating, possible electrostatic effects on moving electrons are discussed in Note 8 in the Supplemental Material [25]. In addition, the possibility of using low-energy electrons could overcome the size limit of conventional free-electron THz sources requiring high-energy electrons [15]. Therefore, our results could provide exciting opportunities for developing miniature free-electron THz radiation sources with high tunability based on graphene plasmonics.

ACKNOWLEDGMENTS

This work was supported by the 973 Program (Grants No. 2013CB632701 and No. 2011CB922004). The research of J.Z. is further supported by the NSFC.

APPENDIX A: SELF-CONSISTENT ELECTROMAGNETIC THEORY

The spectral density of the energy loss suffered by free electrons moving along the x direction atop a graphene layer on a dielectric substrate or a dielectric periodic grating is given by [27]

$$\frac{d}{d\omega}\mathbf{W}_{\mathrm{EEL}} = -\frac{1}{\pi}\int d\mathbf{r}\,\mathrm{Re}\left[\mathbf{J}^{*}(\mathbf{r},\omega)\cdot\mathbf{E}_{x}^{\mathrm{ind}}(\mathbf{r},\omega)\right], \tag{A1}$$

where $\mathbf{E}_x^{\mathrm{ind}}$ is the induced electric field by the electrons. Around GP excitation frequencies ω_{gp}, we assume that $\mathbf{E}_x^{\mathrm{ind}}$ can be expressed in the basis of GP modes as

$$\mathbf{E}_{x}^{\mathrm{ind}}(\mathbf{r},\omega) = \alpha(\omega)\tilde{\mathbf{E}}_{x}(\mathbf{r},\tilde{\omega}_{\mathrm{gp}}) + \mathbf{f}(\omega), \tag{A2}$$

where $\alpha(\omega)$ is the excitation amplitude of GPs, $\tilde{\mathbf{E}}_x(\mathbf{r},\tilde{\omega}_{\mathrm{gp}})$ is the solution of the Helmholtz equation $\nabla^2\tilde{\mathbf{E}}_x(\mathbf{r}) + \frac{\varepsilon(\mathbf{r})}{c^2}\tilde{\omega}_{\mathrm{gp}}^2\tilde{\mathbf{E}}_x(\mathbf{r}) = 0$ imposed with proper boundary conditions (which includes the surface conductivity of graphene), $\tilde{\omega}_{\mathrm{gp}} = \omega_{\mathrm{gp}} - i\kappa$ is the complex eigenfrequency with κ being the damping rate of GPs due to radiative leakage and absorption losses, $\varepsilon(\mathbf{r})$ is the relative permittivity of the structure, c is the light speed in air, and $\mathbf{f}(\omega)$ is a nonresonant background that is assumed to be negligible for $\omega \simeq \omega_{\mathrm{gp}}$.

On the other hand, $\mathbf{E}_x^{\mathrm{ind}}$ can be related to the current density $\mathbf{J}(\mathbf{r},\omega)$ through the inhomogeneous Helmholtz equation

$$\nabla^2\mathbf{E}_{x}^{\mathrm{ind}}(\mathbf{r}) + \frac{\varepsilon(\mathbf{r})}{c^2}\omega^2\mathbf{E}_{x}^{\mathrm{ind}}(\mathbf{r}) = -i\mu_0\omega\mathbf{J}(\mathbf{r},\omega). \tag{A3}$$

By inserting Eq. (A2) and $\mathbf{J}(\mathbf{r},\omega) = \hat{\mathbf{x}}\rho\delta(z-b)e^{i(\omega/v)x}$ to above equation, we obtain

$$\alpha(\omega) = \frac{\rho}{2\varepsilon_0}\frac{\left[\int\tilde{\mathbf{E}}_x^{*}(z=0)e^{i(\omega/v)x}dx\right]\Big/\left[\int\varepsilon(\mathbf{r})|\tilde{\mathbf{E}}_x|^2d\mathbf{r}\right]}{i(\omega-\omega_{\mathrm{gp}})-\kappa}e^{-\gamma_1 b}. \tag{A4}$$

Here, we use the approximation $\omega + \tilde{\omega}_{\mathrm{gp}} \simeq 2\omega_{\mathrm{gp}}$ when $\omega \simeq \omega_{\mathrm{gp}}$. By inserting Eqs. (A2) and (A4) into Eq. (A1), we finally obtain

$$\frac{d}{d\omega}\mathbf{W}_{\mathrm{EEL}} = \frac{\rho^2}{4\pi\varepsilon_0 c}F\frac{\omega_{\mathrm{gp}}^2}{4Q^2(\omega-\omega_{\mathrm{gp}})^2+\omega_{\mathrm{gp}}^2}e^{-2\gamma_1 b}, \tag{A5}$$

where $Q = \omega_{\mathrm{gp}}/2\kappa$, $F = \frac{2}{\pi}\frac{Q}{V/\lambda}$, $V = \frac{\int\varepsilon(\mathbf{r})|\tilde{\mathbf{E}}_x|^2d\mathbf{r}}{|\int\tilde{\mathbf{E}}_x(z=0)e^{-i(\omega/v)x}dx|^2}$, and $\lambda = 2\pi c/\omega_{\mathrm{gp}}$. Note that V is reminiscent of the model volume of optical microcavities describing the spatial confinement of cavity modes [45], and can be understood in terms of a generalized mode volume of GPs describing their spatial confinement. Details on the physical understanding of V is presented in Appendix B.

As mentioned in the main text, the electron energy loss can be assumed to be totally converted into GPs around ω_{gp}. Therefore, in the case of the graphene layer on gratings, the spectral density of the radiated energy can be expressed as

$$\frac{d}{d\omega}\mathbf{W}_{\pm} = \frac{Q}{Q_{r,\pm}}\frac{d}{d\omega}\mathbf{W}_{\mathrm{EEL}}, \tag{A6}$$

where $Q/Q_{r,\pm}$ is the outcoupling factor of GPs to free space toward the air (substrate) side and $Q_{r,\pm}$ is the corresponding radiative quality factor of GPs. By inserting Eq. (A5) into Eq. (A6), and comparing with Eq. (5), we can obtain the Eq. (6) in the main text for the radiation intensity as

$$|R_{\pm}(\omega)|^2 = F\frac{\omega_{\mathrm{gp}}^2}{4Q^2(\omega-\omega_{\mathrm{gp}})^2+\omega_{\mathrm{gp}}^2}\frac{Q}{Q_{r,\pm}}\frac{\sqrt{\varepsilon_{\pm}}}{\cos(\theta_{\pm})}.$$

APPENDIX B: PHYSICAL UNDERSTANDING OF V DEFINED IN EQS. (6) AND (A5)

For optical microcavities which support cavity modes, the mode volume V_{cav} defined as [45]

$$V_{\mathrm{cav}} = \frac{\int\varepsilon(\mathbf{r})|\tilde{\mathbf{E}}_{\mathrm{cav}}(\mathbf{r})|^2d\mathbf{r}}{\varepsilon(\mathbf{r}_c)|\tilde{\mathbf{E}}_{\mathrm{cav}}(\mathbf{r}_c)|^2d\mathbf{r}} \tag{B1}$$

describes the spatial confinement of light in the cavity, where $\varepsilon(\mathbf{r})$ is the relative permittivity of the cavity, $\tilde{\mathbf{E}}_{\mathrm{cav}}$ is the electric field distribution of the cavity mode, and $\mathbf{r}_c$ is the antinode of the electric field. The mode volume V_{cav} is connected to the enhancement of the spontaneous emission rate of a quantum emitter at $\mathbf{r}_c$ in a optical cavity, which is proportional to $Q_{\mathrm{cav}}/V_{\mathrm{cav}}$, with Q_{cav} being the quality factor of the cavity. From a fundamental point of view, $Q_{\mathrm{cav}}/V_{\mathrm{cav}}$ is related to the

photonic local density of states probed by the emitter at $\mathbf{r}_c$ in the cavity.

In Eq. (6), to describe the enhancement of electron energy losses experienced by moving electrons atop a graphene layer, we introduce the quantity V for GP modes as

$$V = \frac{\int \varepsilon(\mathbf{r})|\tilde{\mathbf{E}}_x|^2 d\mathbf{r}}{|\int \tilde{\mathbf{E}}_x(z=0)e^{-i(\omega/v)x}dx|^2}. \tag{B2}$$

Note that $\tilde{\mathbf{E}}_x(k_x; z=0) \equiv \int \tilde{\mathbf{E}}_x(z=0)e^{-i(\omega/v)x}dx$ is the amplitude of the electric field $\tilde{\mathbf{E}}_x(z=0)$ decomposed into parallel wave vector $k_x = \omega/v$. Therefore, Eq. (B2) can be rewritten as

$$V = \frac{\int \varepsilon(\mathbf{r})|\tilde{\mathbf{E}}_x|^2 d\mathbf{r}}{|\tilde{\mathbf{E}}_x(k_x; z=0)|^2}. \tag{B3}$$

By comparing Eq. (B3) with Eq. (B1), and noting that the enhancement of the electron energy loss is proportional to Q/V, V can be understood in terms of a generalized mode volume of GPs, describing the spatial confinement of GPs. Moreover, it can be analytically showed that V is closely related to the lateral confinement of GPs for a graphene layer on a dielectric substrate (see Note 4 in the Supplemental Material [25]). However, since the electrons are moving uniformly along the x direction, they are delocalized in the real space along the x direction, but localized in the momentum space at a specific wave vector $k_x = \omega/v$. Therefore, the definition of V in Eq. (B3) involves the electric field at $k_x = \omega/v$ and $z = 0$. It is interesting to point out that Q/V here is actually related to the photonic local density of states probed by moving electrons at a specific wave vector along the x direction and a specific position along the z direction [46].

APPENDIX C: OBTAINING Q, V/λ, AND $Q/Q_{r,\pm}$ BY FITTING TO NUMERICAL RESULTS

The processes to obtain these parameters can be summarized as follows. First, we fit numerical results of the radiation intensity to Eq. (6) and obtain the quality factor Q. In general, $1/Q = 1/Q_r + 1/Q_{nr}$, where Q_r and Q_{nr} are the radiative and nonradiative contribution to Q, respectively. By varying the relaxation time τ in graphene, it is found that Q_r is nearly constant and $Q_{nr} = A\omega_{\rm gp}\tau$, with A being a constant for specific $\omega_{\rm gp}$. In the limit of $\tau \to \infty$, we can obtain Q_r. In the case that excited GPs can couple to free space toward both sides, using $|R_+(\omega_{\rm gp})|^2/|R_-(\omega_{\rm gp})|^2 = \frac{\sqrt{\varepsilon_+}/\cos(\theta_+)}{\sqrt{\varepsilon_-}/\cos(\theta_-)}\frac{Q_{r,-}}{Q_{r,+}}$ from Eq. (6) and $1/Q_r = 1/Q_{r,+} + 1/Q_{r,-}$, we can obtain $Q_{r,+}$ and $Q_{r,-}$ from Q_r. With Q and $Q/Q_{r,\pm}$, we can finally obtain V/λ from Eq. (6) at $\omega = \omega_{\rm gp}$. Details are presented in Note 6 in the Supplemental Material [25].

[1] F. Bonaccorso, Z. Sun, T. Hasan, and A. C. Ferrari, Nat. Photonics **4**, 611 (2010).
[2] A. K. Geim and K. S. Novoselov, Nat. Mater. **6**, 183 (2007).
[3] B. Wunsch, T. Stauber, F. Sols, and F. Guinea, New J. Phys. **8**, 318 (2006).
[4] E. H. Hwang and S. Das Sarma, Phys. Rev. B **75**, 205418 (2007).
[5] W. L. Barnes, A. Dereux, and T. W. Ebbesen, Nature (London) **424**, 824 (2003).
[6] M. Jablan, H. Buljan, and M. Soljačić, Phys. Rev. B **80**, 245435 (2009).
[7] F. H. L. Koppens, D. E. Chang, and F. J. García de Abajo, Nano Lett. **11**, 3370 (2011).
[8] A. N. Grigorenko, M. Polini, and K. S. Novoselov, Nat. Photonics **6**, 749 (2012).
[9] A. Vakil and N. Engheta, Science **332**, 1291 (2011).
[10] L. Ju, B. Geng, J. Horng, C. Girit, M. Martin, Z. Hao, H. A. Bechtel, X. Liang, A. Zettl, Y. R. Shen, and F. Wang, Nat. Nanotechnol. **6**, 630 (2011).
[11] S. Thongrattanasiri, F. H. L. Koppens, and F. J. García de Abajo, Phys. Rev. Lett. **108**, 047401 (2012).
[12] S. Thongrattanasiri and F. J. García de Abajo, Phys. Rev. Lett. **110**, 187401 (2013).
[13] M. Gullans, D. E. Chang, F. H. L. Koppens, F. J. García de Abajo, and M. D. Lukin, Phys. Rev. Lett. **111**, 247401 (2013).
[14] M. Tonouchi, Nat. Photonics **1**, 97 (2007).
[15] G. P. Gallerano and S. Biedron, in *Proceedings of the 2004 FEL Conference*, Trieste, Italy, 2004, p. 216, http://accelconf.web.cern.ch/accelconf/f04/papers/FRBIS02/FRBIS02.PDF.
[16] S. J. Smith and E. M. Purcell, Phys. Rev. **92**, 1069 (1953).
[17] A. M. Cook, R. Tikhoplav, S. Y. Tochitsky, G. Travish, O. B. Williams, and J. B. Rosenzweig, Phys. Rev. Lett. **103**, 095003 (2009).
[18] P. G. O'Shea and H. P. Freund, Science **292**, 1853 (2001).
[19] K. Kan *et al.*, Appl. Phys. Lett. **99**, 231503 (2011).
[20] G. Andonian *et al.*, Appl. Phys. Lett. **98**, 202901 (2011).
[21] G. Adamo, K. F. MacDonald, Y. H. Fu, C-M. Wang, D. P. Tsai, F. J. García de Abajo, and N. I. Zheludev, Phys. Rev. Lett. **103**, 113901 (2009).
[22] G. Robb, Nat. Nanotechnol. **4**, 707 (2009).
[23] S. Liu, M. Hu, Y. Zhang, W. Liu, P. Zhang, and J. Zhou, Phys. Rev. E **83**, 066609 (2011).
[24] S. Liu, P. Zhang, W. Liu, S. Gong, R. Zhong, Y. Zhang, and M. Hu, Phys. Rev. Lett. **109**, 153902 (2012).
[25] See Supplemental Material at http://link.aps.org/supplemental/10.1103/PhysRevB.89.245434 for further details on the derivation of Eqs. (2) and (5), validation of the self-consistent theory, tunability of radiation emission from GPs by engineering the grating structure, a discussion on the influence of the relaxation time in graphene, and possible electrostatic effects on the moving electrons in the case of electrostatic doping.
[26] L. D. Landau, E. M. Liftshitz, and L. P. Pitaevskii, *Electrodynamics of Continuous Media* (Pergamon, Oxford, UK, 1984).
[27] F. J. García de Abajo, Rev. Mod. Phys. **82**, 209 (2010).
[28] F. J. García de Abajo, ACS Nano **7**, 11409 (2013).
[29] P. M. van den Berg, J. Opt. Soc. Am. **63**, 689 (1973).
[30] S. Yamaguti, J.-I. Inoue, O. Haeberlé, and K. Ohtaka, Phys. Rev. B **66**, 195202 (2002).
[31] F. J. García de Abajo and L. A. Blanco, Phys. Rev. B **67**, 125108 (2003).

[32] T. R. Zhan, X. Shi, Y. Y. Dai, X. H. Liu, and J. Zi, J. Phys.: Condens. Matter **25**, 215301 (2013).
[33] T. R. Zhan, F. Y. Zhao, X. H. Hu, X. H. Liu, and J. Zi, Phys. Rev. B **86**, 165416 (2012).
[34] Y. Hao, M. S. Bharathi, L. Wang, Y. Liu, H. Chen, S. Nie, X. Wang, H. Chou, C. Tan, B. Fallahazad, H. Ramanarayan, C. W. Magnuson, E. Tutuc, B. I. Yakobson, K. F. McCarty, Y.-W. Zhang, P. Kim, J. Hone, L. Colombo, and R. S. Ruoff, Science **342**, 720 (2013).
[35] J.-H. Chen, C. Jang, S. Xiao, M. Ishigami, and M. S. Fuhrer, Nat. Nanotechnol. **3**, 206 (2008).
[36] K. I. Bolotin, K. J. Sikes, Z. Jiang, M. Klima, G. Fudenberg, J. Hone, P. Kim, and H. L. Stormer, Solid State Commun. **146**, 351 (2008).
[37] C. R. Dean, A. F. Young, I. Meric, C. Lee, L. Wang, S. Sorgenfrei, K. Watanabe, T. Taniguchi, P. Kim, K. L. Shepard, and J. Hone, Nat. Nanotechnol. **5**, 722 (2010).
[38] H. Yan, T. Low, W. Zhu, Y. Wu, M. Freitag, X. Li, F. Guinea, P. Avouris, and F. Xia, Nat. Photonics **7**, 394 (2013).
[39] W. Gao, G. Shi, Z. Jin, J. Shu, Q. Zhang, R. Vajtai, P. M. Ajayan, J. Kono, and Q. Xu, Nano Lett. **13**, 3698 (2013).
[40] A. J. McCulloch, D. V. Sheludko, M. Junker, and R. E. Scholten, Nat. Commun. **4**, 1692 (2013).
[41] P. Hommelhoff, Y. Sortais, A. Aghajani-Talesh, and M. A. Kasevich, Phys. Rev. Lett. **96**, 077401 (2006).
[42] B. J. Siwick, J. R. Dwyer, R. E. Jordan, and R. J. D. Miller, Science **302**, 1382 (2003).
[43] W. E. King, G. H. Campbell, A. Frank, B. Reed, J. F. Schmerge, B. J. Siwick, B. C. Stuart, and P. M. Weber, J. Appl. Phys. **97**, 111101 (2005).
[44] S. E. Korbly, A. S. Kesar, J. R. Sirigiri, and R. J. Temkin, Phys. Rev. Lett. **94**, 054803 (2005).
[45] K. J. Vahala, Nature (London) **424**, 839 (2003).
[46] F. J. García de Abajo and M. Kociak, Phys. Rev. Lett. **100**, 106804 (2008).